

1 **Supplementary Figure Captions**

2

3 **Supp. Fig. 1** Detailed stratigraphic sections BS-02 and BS-03 showing correlations. The basal meter of
4 these sections are shown in more detail in Figure 4 and contain two distinctive breccia units. The
5 overlying sections are mostly laminated black chert with some thin graded ashy-to-carbonaceous beds.
6 Both sections are interrupted by vertical and stratiform black chert dikes, in some cases containing
7 angular clasts of laminated to massive grey chert. Both sections are capped by several meters of whitish
8 to light grey silicified ash immediately overlying bright green silicified ash layers.

9

10 **Supp. Fig. 2** Detailed stratigraphic section SAF 187.

11

12 **Supp. Fig. 3** Detailed stratigraphic section SAF 191.

13

14 **Supp. Fig. 4** Detailed stratigraphic section SAF 186.

15

16 **Supp. Fig. 5** Detailed stratigraphic section SAF 625.

17

18 **Supp. Fig. 6** Detailed stratigraphic section BM-01.

19

20 **Supp. Fig. 7** Detailed stratigraphic section SAF 620, upper 16 m.

21

22 **Supp. Fig. 8** Detailed stratigraphic section CQ-01.

23

24 **Supp. Fig. 9.** Representative Raman spectra of putative carbonaceous matter from upper Mendon
25 Formation samples. Spectra show two peaks characteristic of partially disordered carbonaceous material.
26 Calculated ratios of peak areas are shown on the right edge of each spectrum. Petrographic texture
27 abbreviations: L – laminated carbonaceous intraclasts, F – fine-grained carbonaceous material, and A –
28 composite carbonaceous grain.

29
30 **Supp. Fig. 10** Thin section photomicrographs of composite carbonaceous grains. (a) Composite
31 carbonaceous grains surrounded by isopachous silica cement. (b) “Sandstone” composed entirely of fine-
32 sand sized simple and composite carbonaceous grains.

33
34 **Supp. Fig. 11** Photomicrographs of laminated carbonaceous intraclasts. (a) Somewhat diffusely laminated
35 intraclast with small domal structures (arrows) with geometries analogous to botryoidal precipitates. (b)
36 Mostly planar laminations with steep truncation surface (arrow). (c) Example showing relatively thick
37 microquartz cement layers (arrows) precipitated in between organic-rich laminations.

38
39 **Supp. Fig. 12** Photomicrographs of non-laminated carbonaceous intraclasts in plane polarized light (PPL, a,
40 c) and cross-polarized transmitted light (XPL, b, d).

41
42 **Supp. Fig. 13** Photomicrographs of fine *in situ* carbonaceous laminations. (a) Thin, somewhat
43 anastomosing carbonaceous laminations separated by thicker layers of relatively pure microquartz from a
44 sample of banded ferruginous chert. (b) Thin, even carbonaceous laminations separated by thicker
45 microquartz layers.

46

47 **Supp. Fig. 14** Fine- to medium-sand sized volcanic sand grains – aggregates of microquartz and
48 phyllosilicates. Some grains have fine carbonaceous coatings.

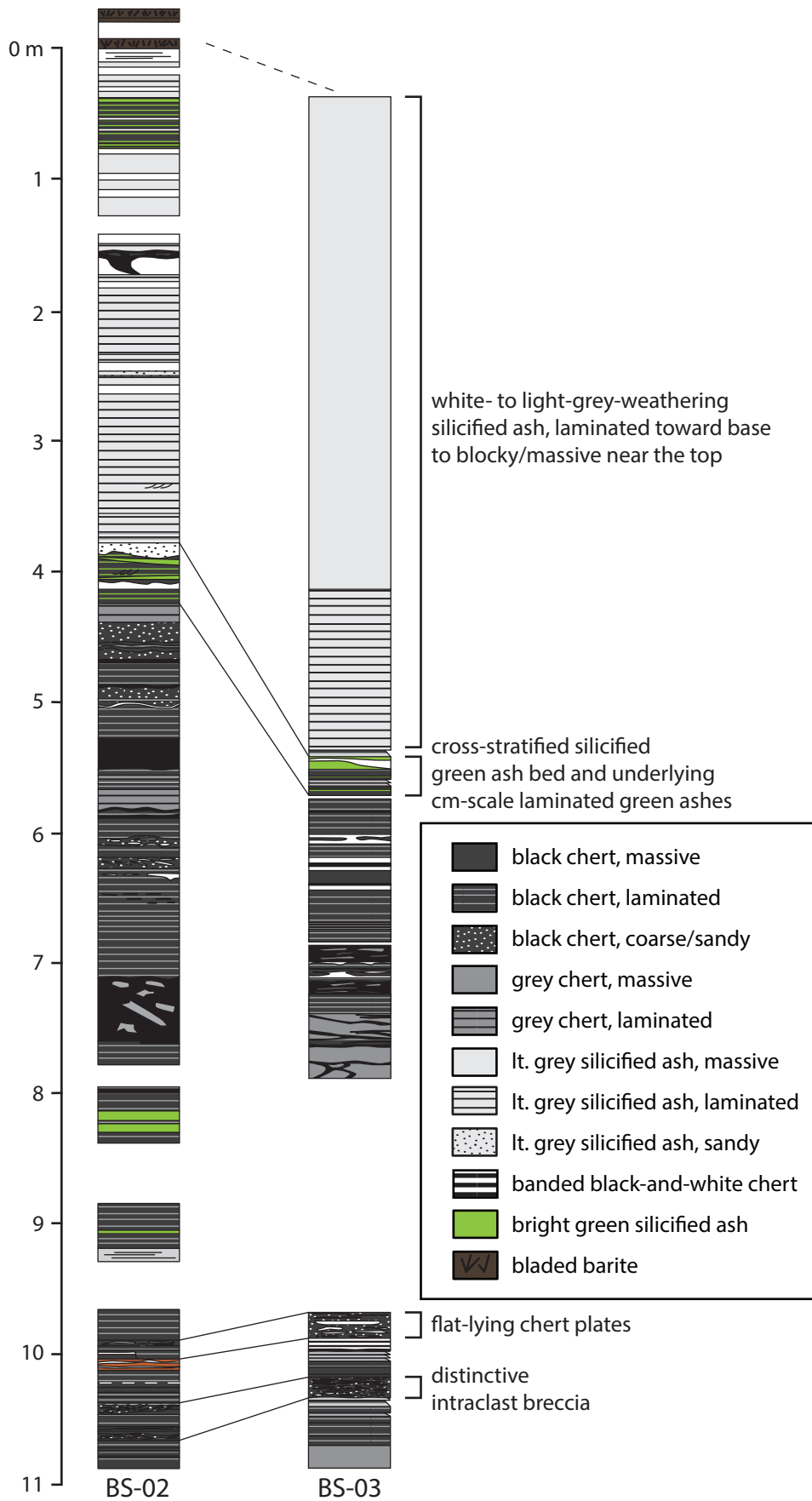
49

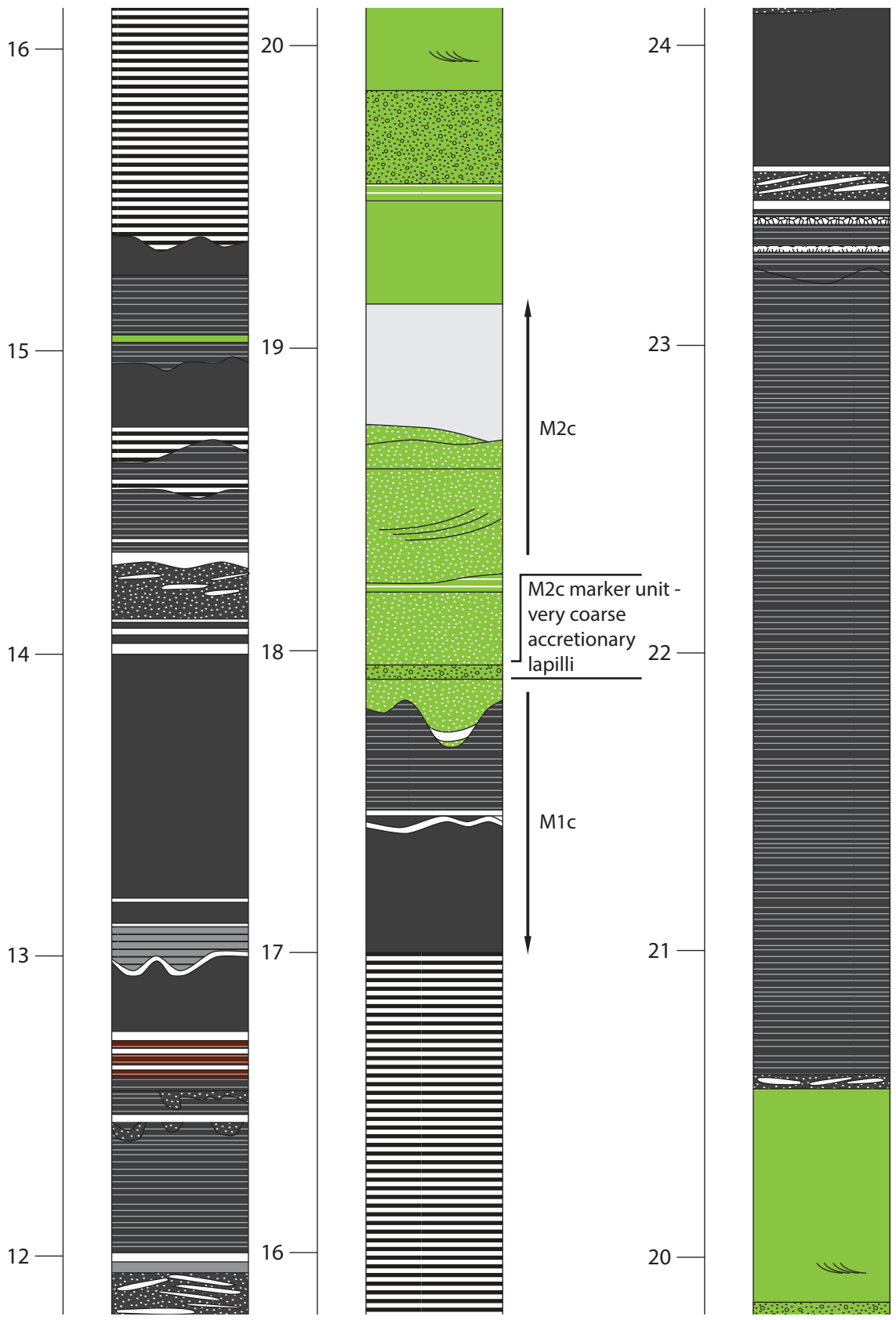
50 **Supp. Fig. 15** White chert band composed of moderately-compacted silica granules and adjacent to
51 carbonaceous black chert layers.

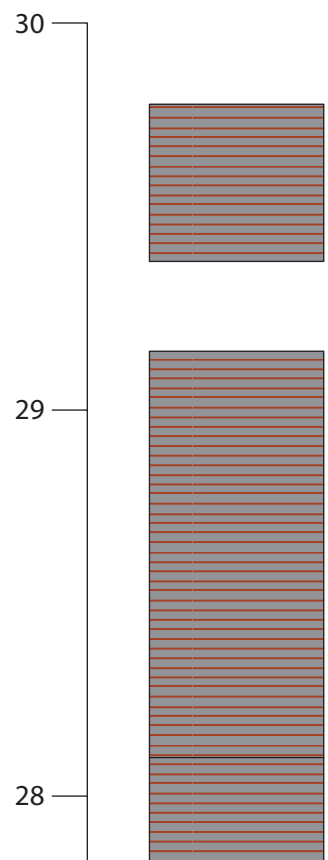
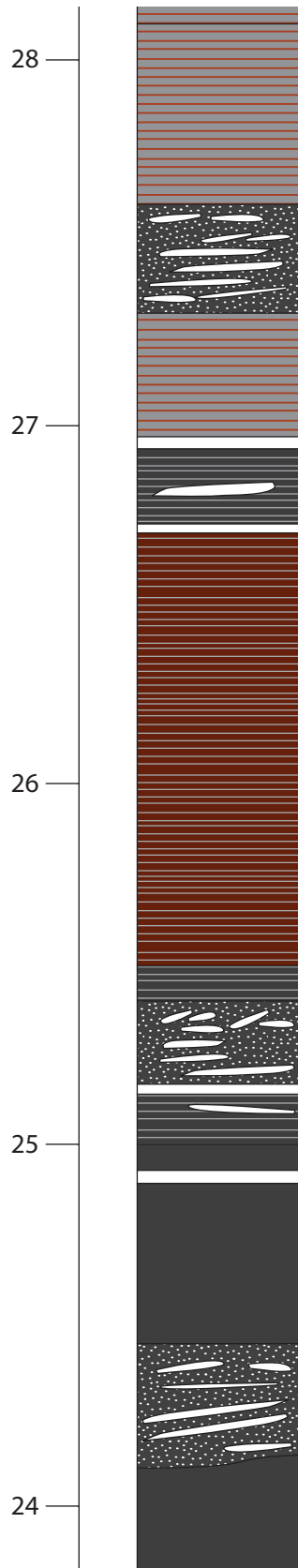
52

53 **Supp. Fig. 16** Thin section photomicrograph of wispy edge of white chert band, suggesting that it was still
54 relatively soft and deformable, rather than rigidly cemented.

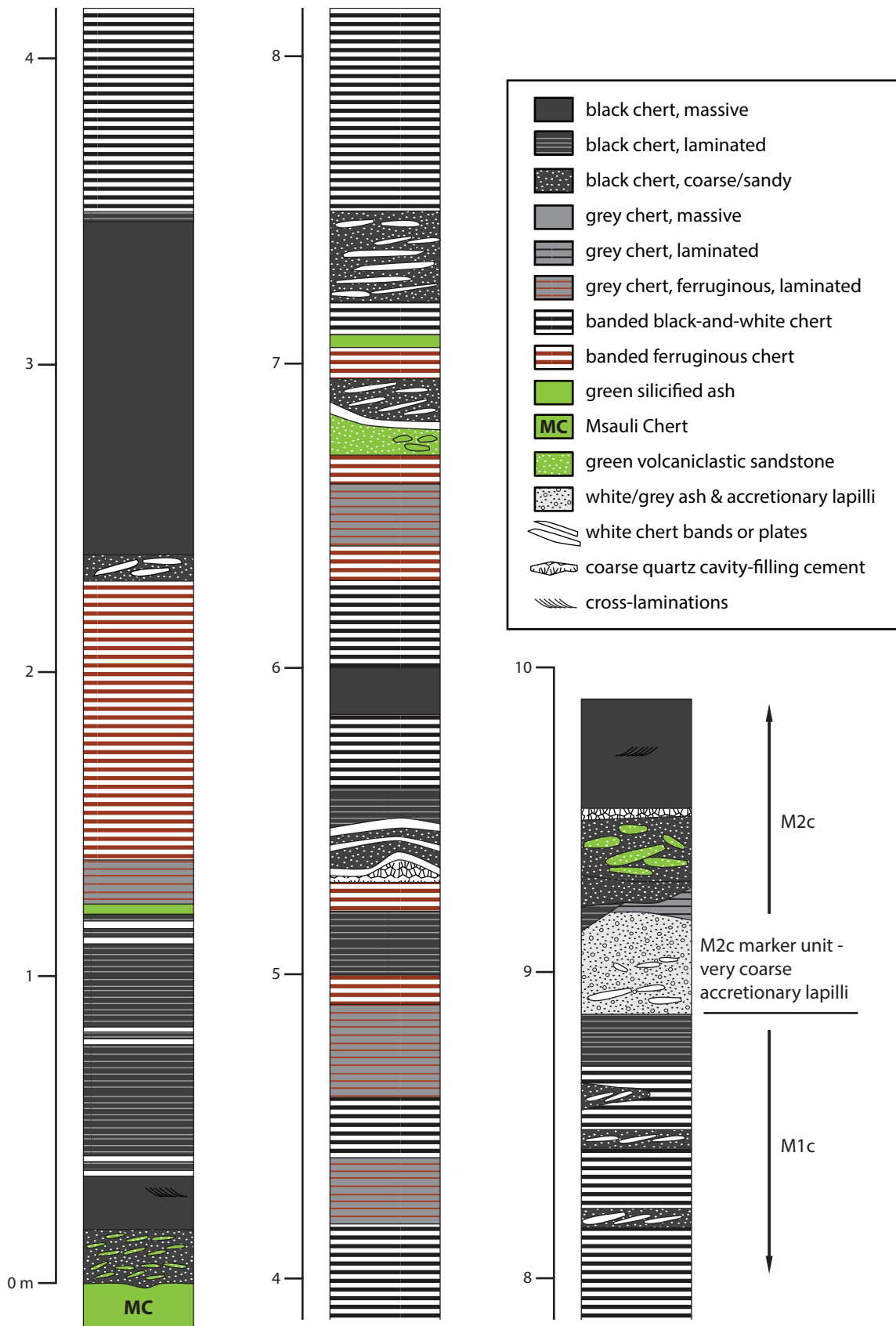
Supplementary Figure S1



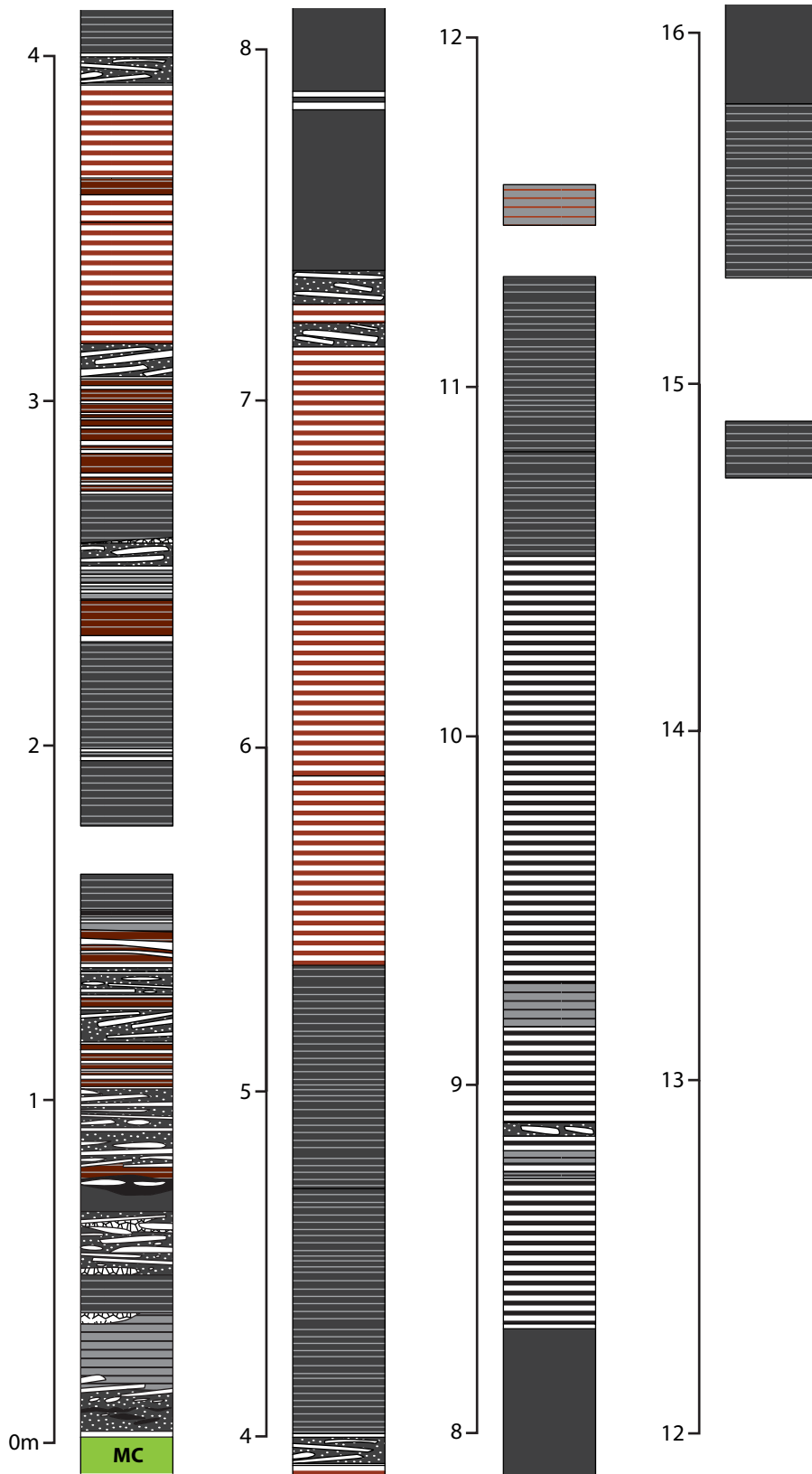


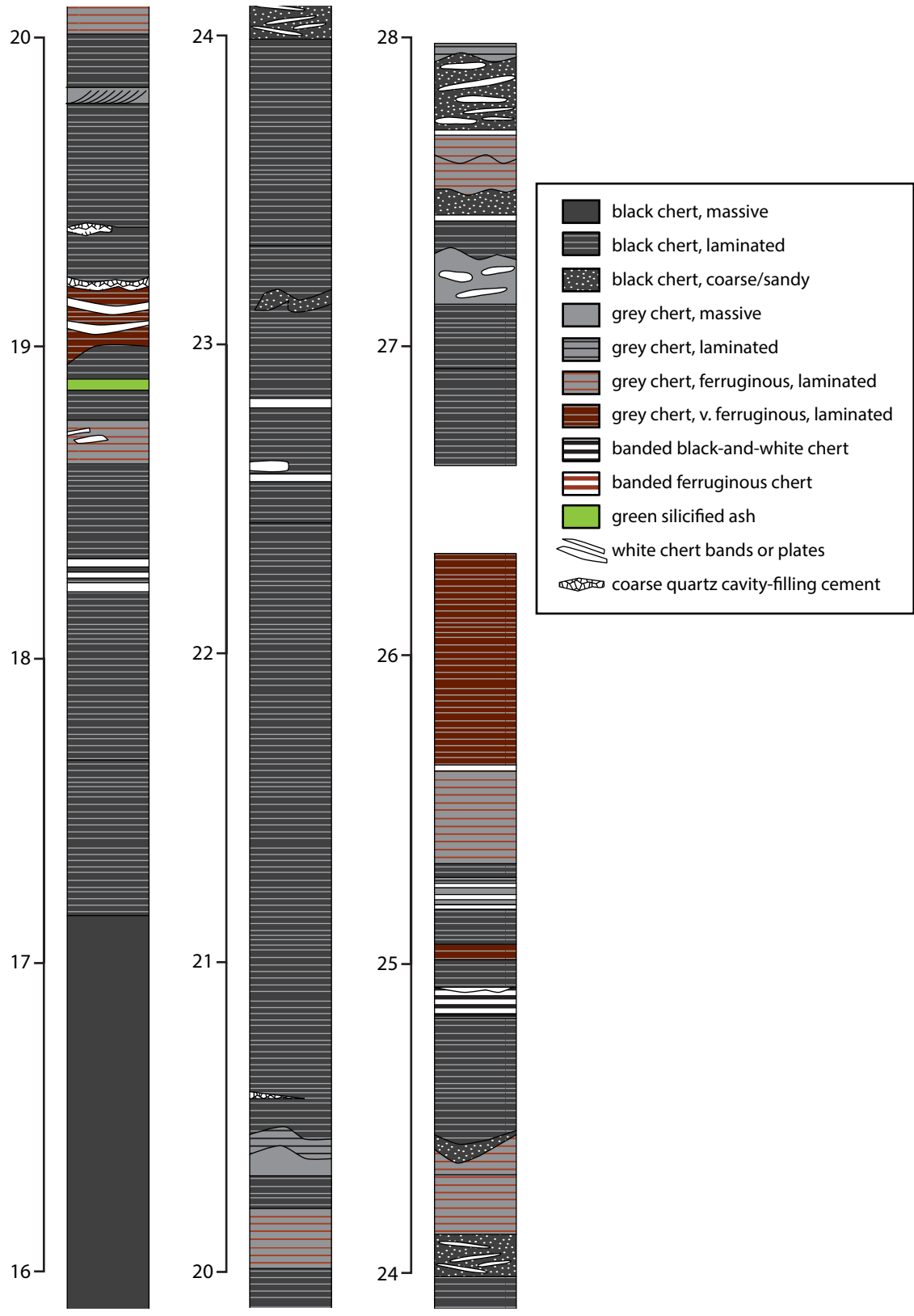


Supplementary Figure S3

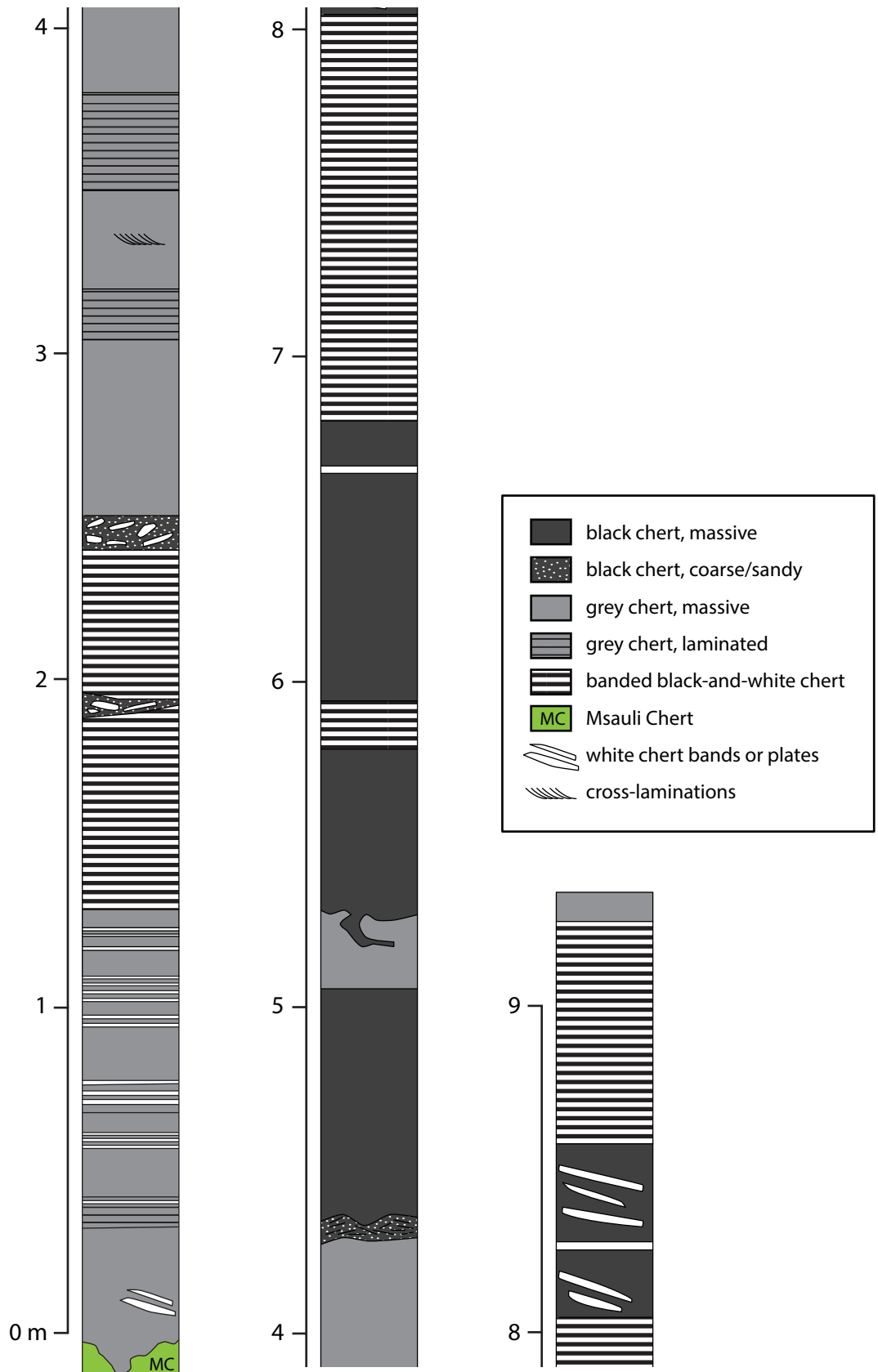


Supplementary Figure S4

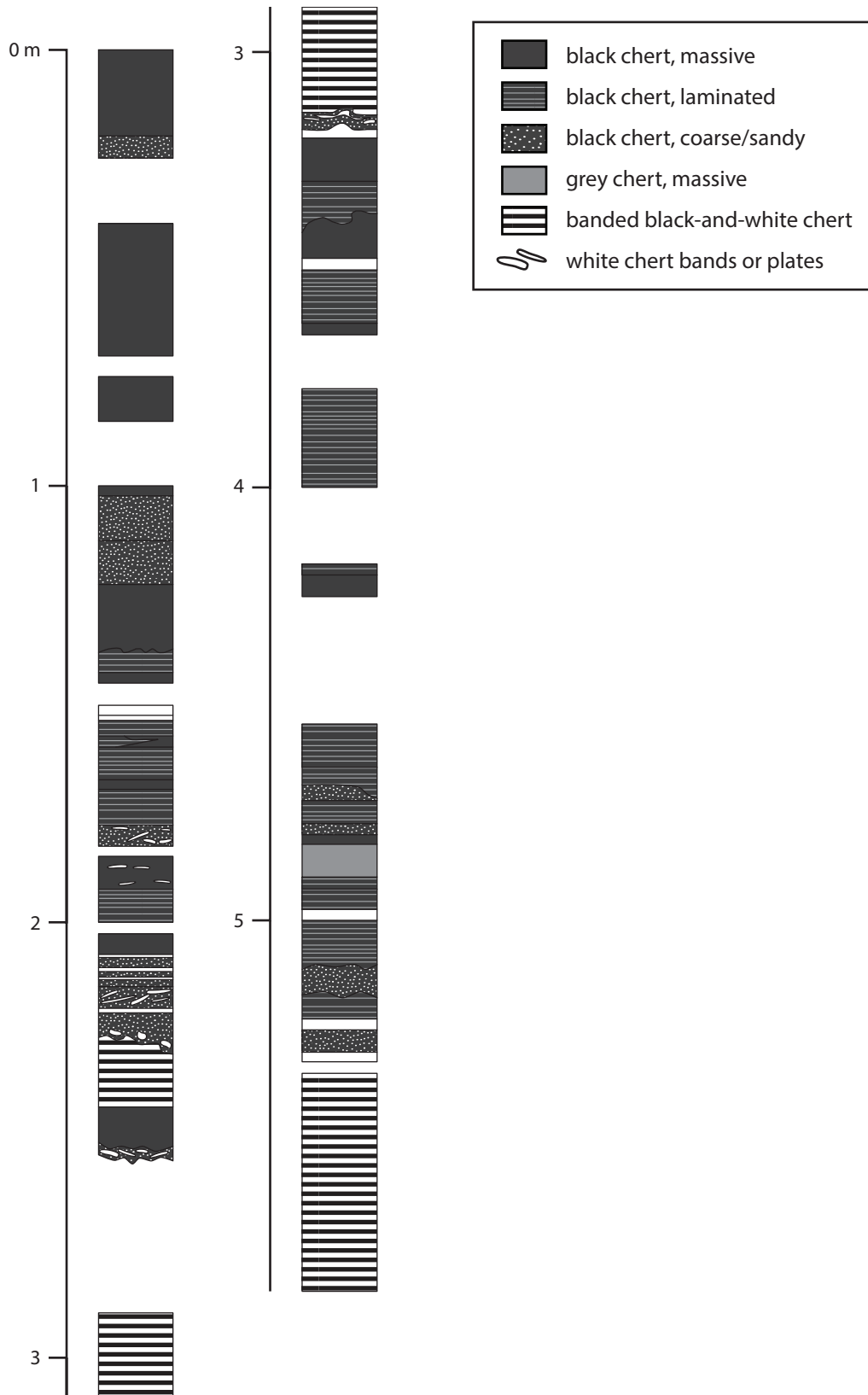




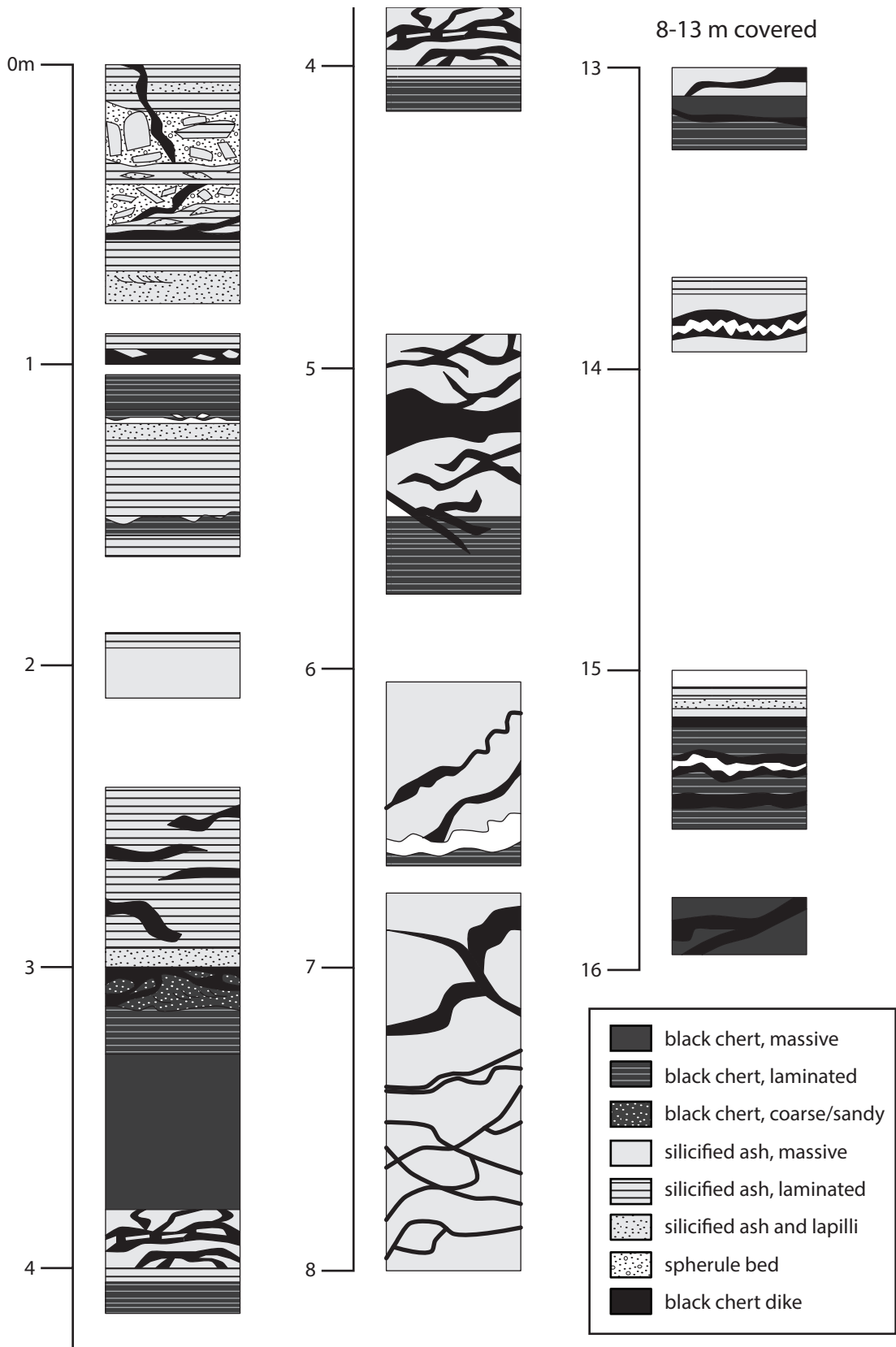
Supplementary Figure S5



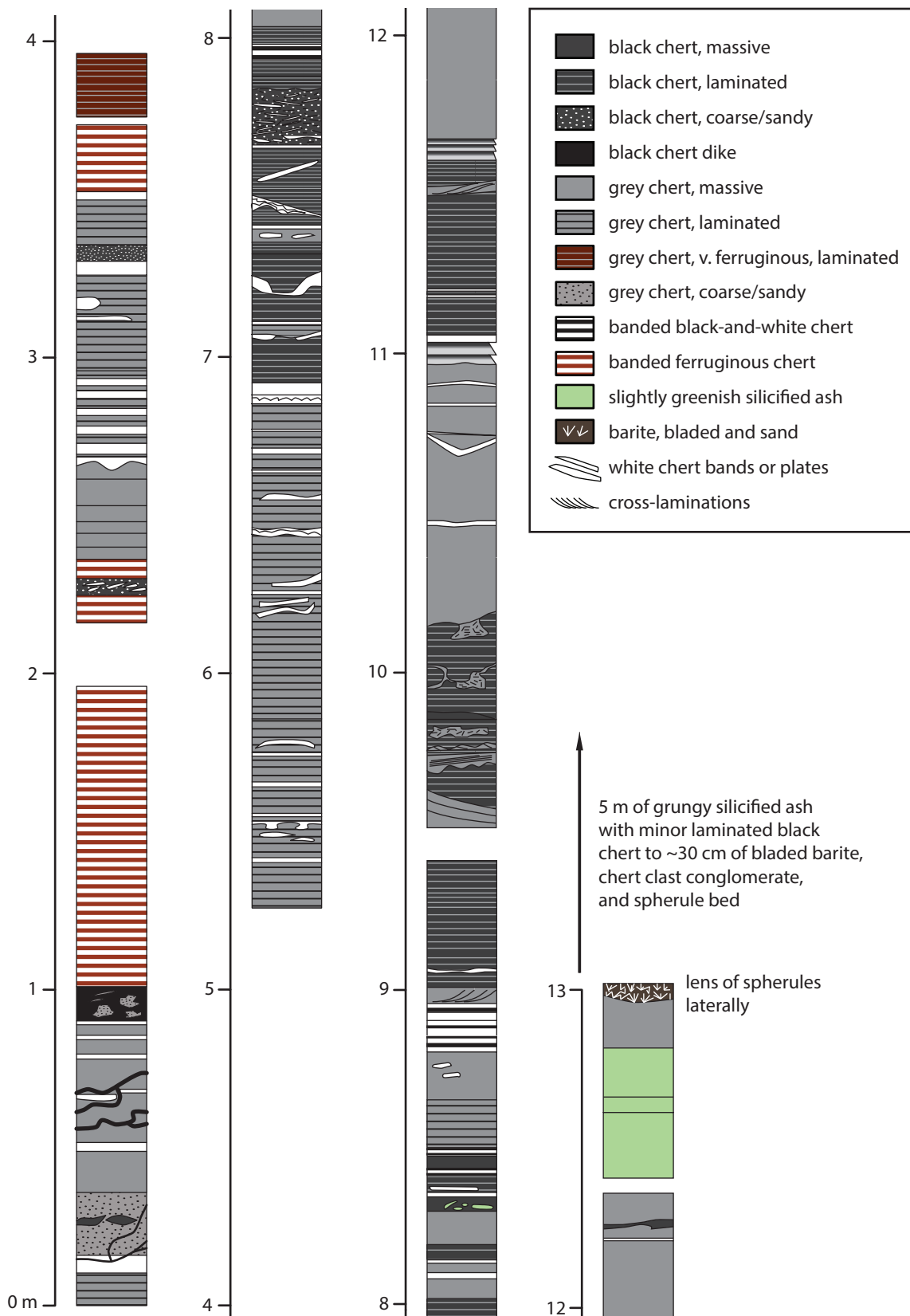
Supplementary Figure S6



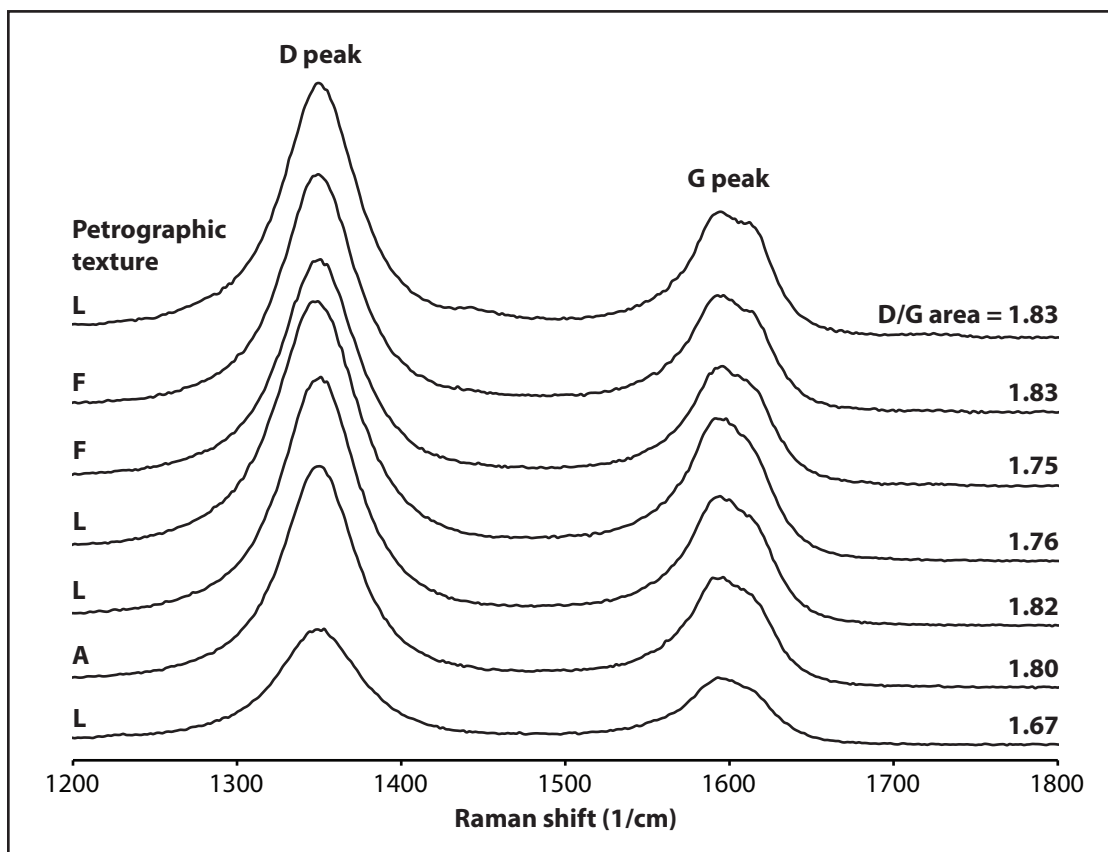
Supplementary Figure S7



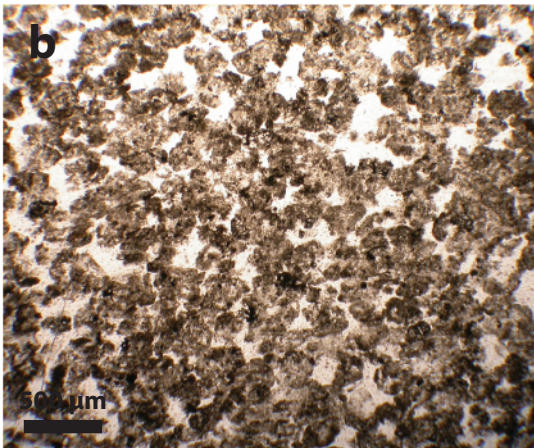
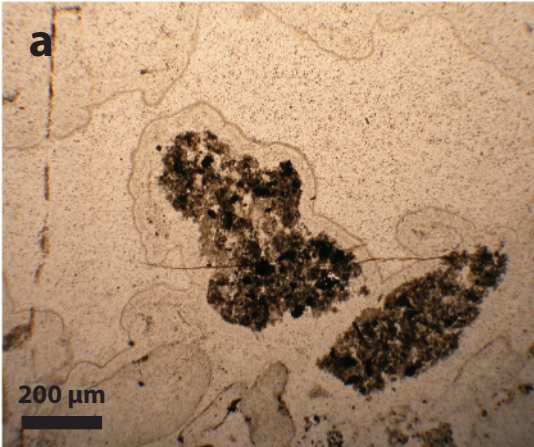
Supplementary Figure S8



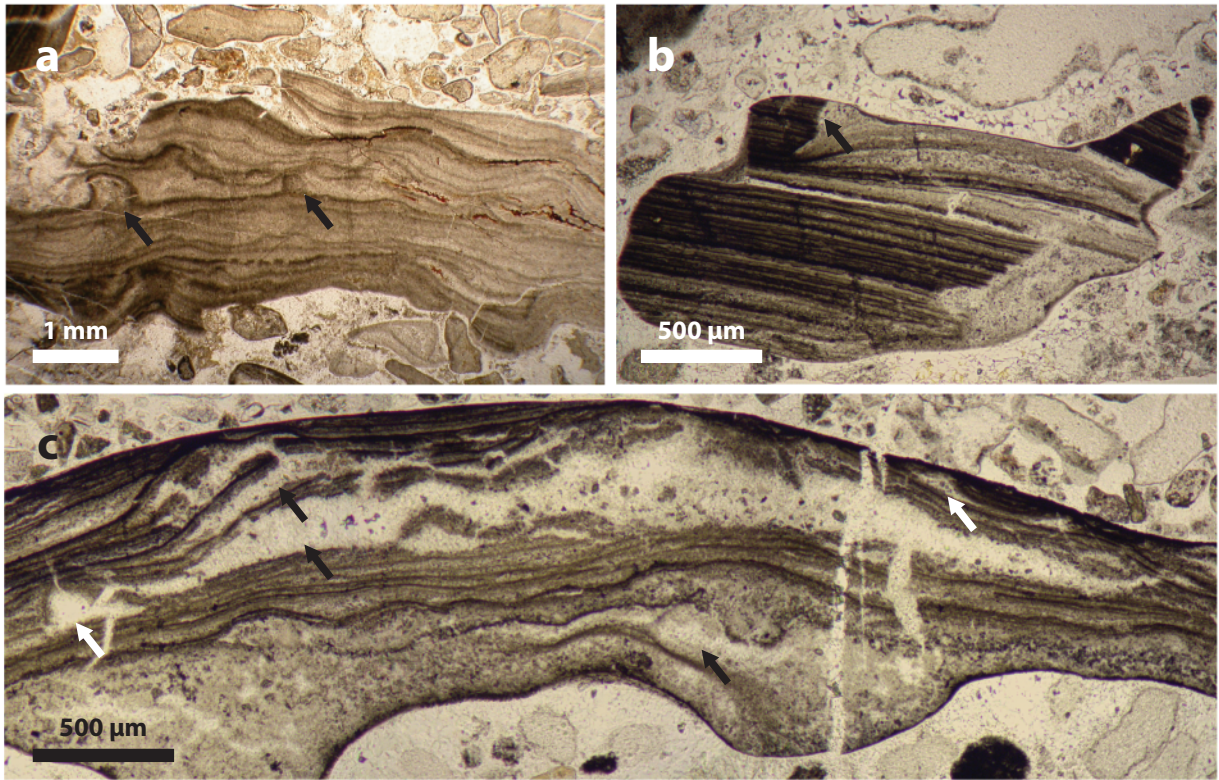
Supplementary Figure S9



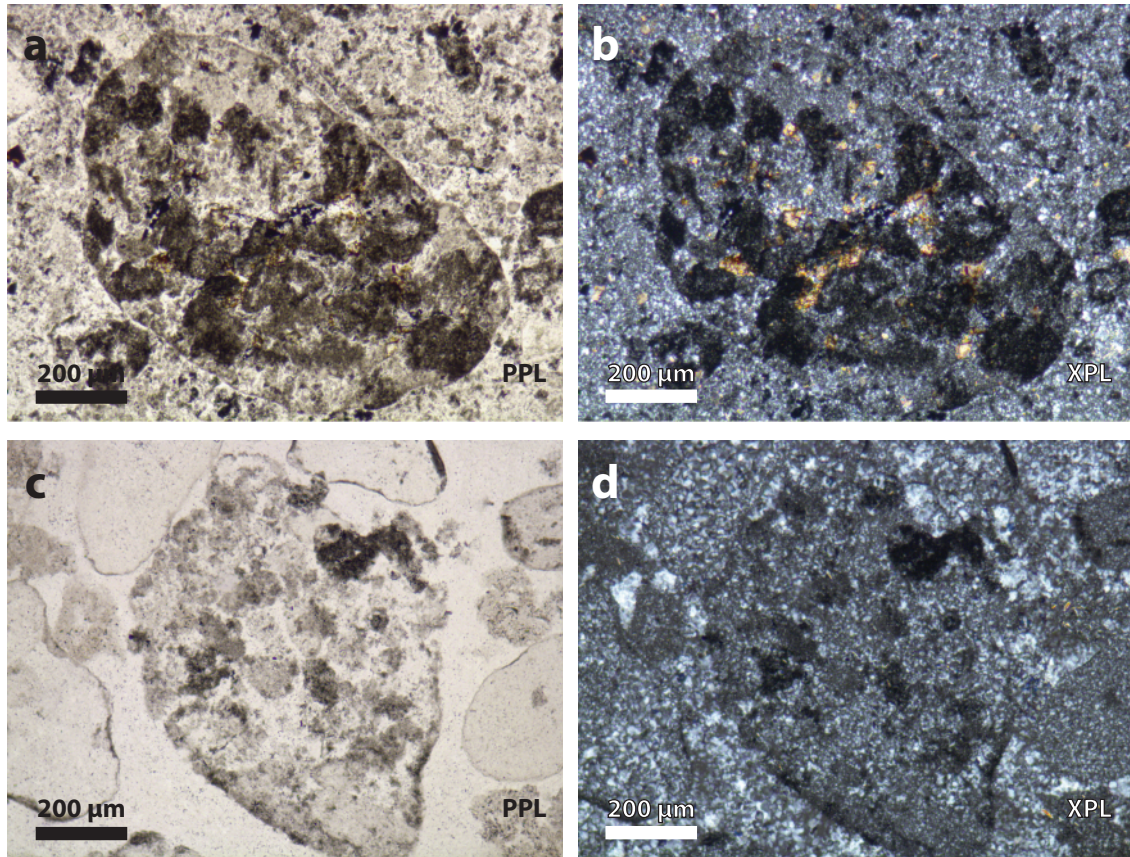
Supplementary Figure S10



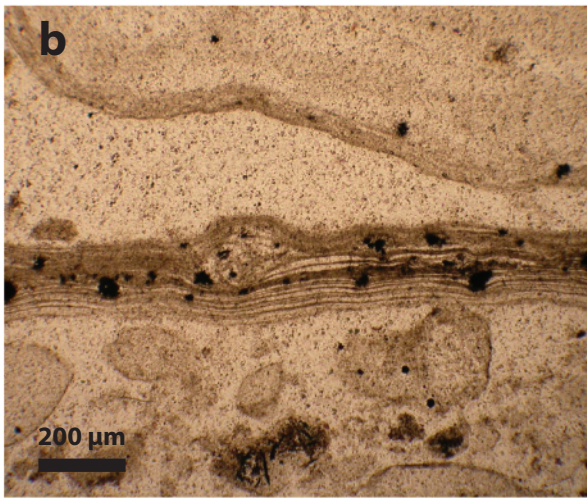
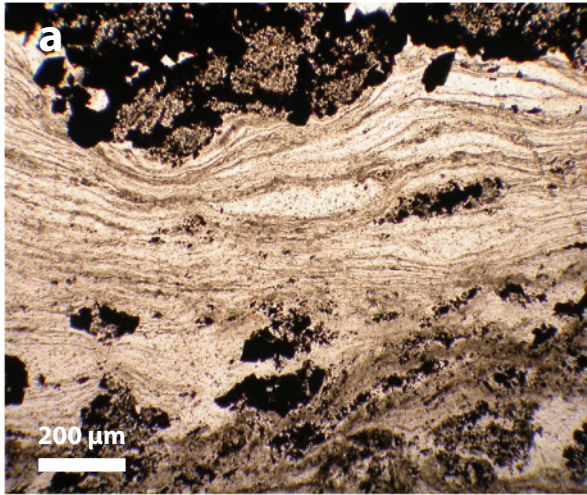
Supplementary Figure S11



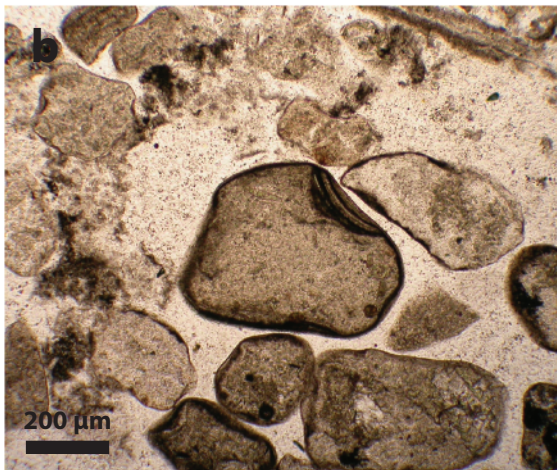
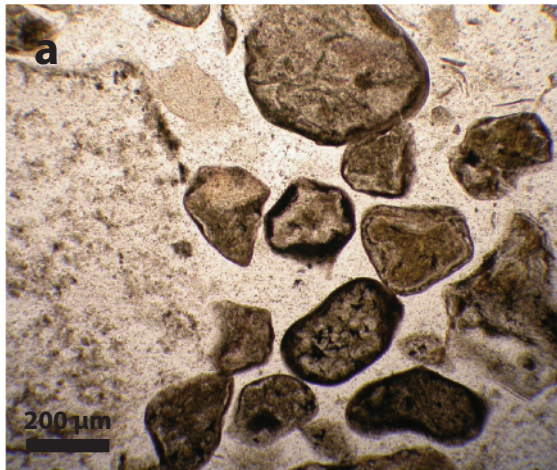
Supplementary Figure S12



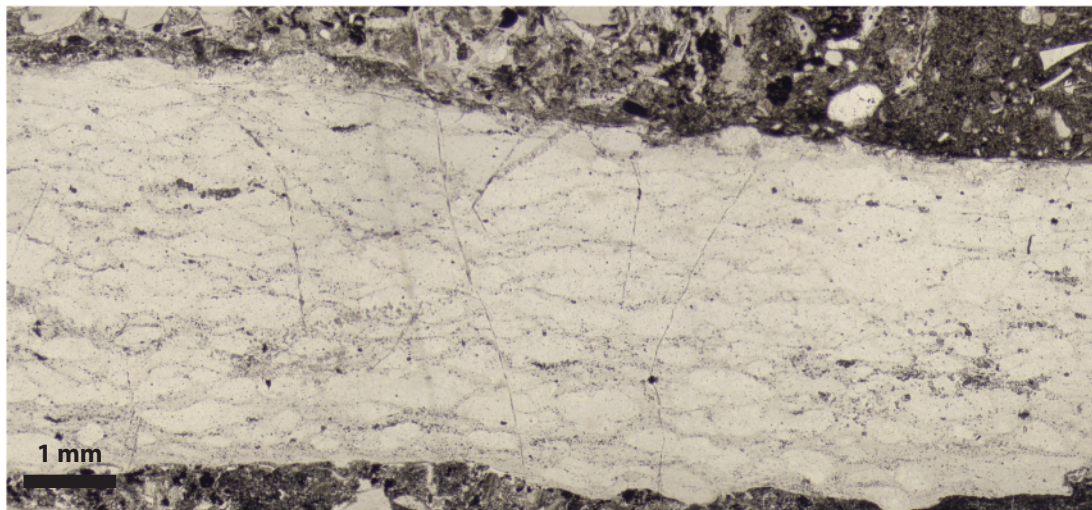
Supplementary Figure S13



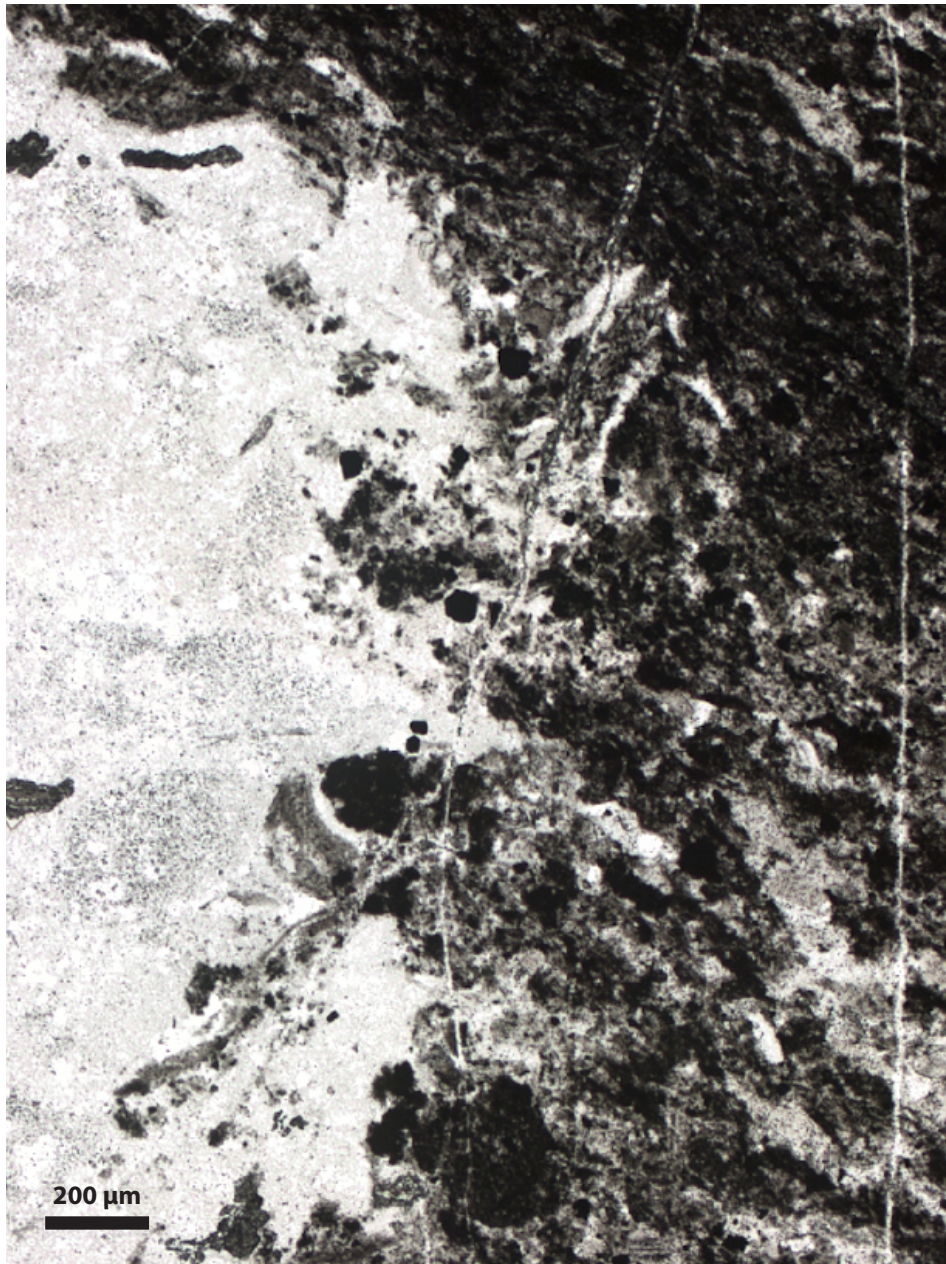
Supplementary Figure S14



Supplementary Figure S15



Supplementary Figure S16



Supplementary Table S1 – Stratigraphic sections

Stratigraphic section ^a	Mendon cycle	Latitude ^b	Longitude ^b	Figure(s)
BH-03	M2c? ^c	S 25° 54.916'	E 30° 55.962'	6
SAF 186	M1c, M2c	S 25° 55.026'	E 30° 56.089'	6, S4
SAF 187	M1c, M2c	S 25° 54.950'	E 30° 57.967'	6, S2
SAF 625	M1c, M2c	S 25° 54.951'	E 30° 58.300'	6, S5
SAF 191	M1c, M2c	S 25° 55.024'	E 30° 58.955'	6, S3
SAF 521	M3c2	S 25° 54.037'	E 31° 0.361'	7
BS-02	M4c	S 25° 54.508	E 31° 3.232'	4, 7, S1
BS-03	M4c	S 25° 54.814'	E 31° 3.262'	4, 7, S1
BM-01	M5c	S 25° 53.218	E 31° 3.416	7, S6
SAF 620	M5c	S 25° 52.753'	E 31° 4.884'	7, S7
CQ-01	M5c	S 25° 52.953	E 31° 6.221'	7, S8
BHR-01	M3c? ^d	S 25° 56.648'	E 31° 6.428'	7

^aSections are listed from west to east.

^bWGS 84 reference datum.

^cSection is separated from the following M2c sections by a fault and the base is not preserved, so there is some uncertainty as to whether this section is also M2c.

^dSection is faulted out at the base, so it is difficult to determine how many cycles it overlies. It could be M2c, but more likely M3c.

Supplementary Table S2 – Intraclast breccia point count classification

	Point count grain categories	Overall Percentage
Carbonaceous grains	Simple grain	7.4
	Composite grain	4.2
	Laminated intraclast	6.4
	Non-laminated intraclast	7.7
Volcanic grains	Lapilli	0 ^a
	Aggregate of lapilli	0 ^a
	Other volcanic	9.1
Silica granules, etc.	Granule	3.1
	Aggregate of granules	7.0
	Other chert grain (e.g. chert plate)	16.5
Other grains	Quartz grain	0 ^a
	Impact spherule	0 ^a
	Opaque grain	0.6
Matrix/cements	Carbonaceous matrix	12.2
	Chert matrix/cement	25.6

^aAt least one instance (and in some cases multiple instances) of this grain type were observed, but the overall abundance is not significantly different from zero.

Supplementary Table S3 – Geochemical sample locations

Sample	Lithology	Formation	Latitude	Longitude	Source	Locality
SAF 23-195	BBWC	Kromberg	S 26° 1.709'	E 30° 59.414'	Lowe, 1999	SAF 23
SAF 521-3	BBWC	Mendon	S 25° 54.037'	E 31° 0.361'	This study	Umba Umba
SAF 521-10	BBWC	Fig Tree	S 25° 54.037'	E 31° 0.361'	This study	Umba Umba
MW-41-2	BBWC	Mendon	S 25° 54.167'	E 30° 57.167'	Walsh, 1989	Barite E
SAF 199-10	BBWC	Mendon	S 25° 54.900'	E 30° 55.967'	This study	Bruce's Hill
MW-43-1	Massive black cht.	Mendon	S 25° 54.500'	E 31° 3.750'	This study	MW-43
SAF 115-3	Massive black cht.	Fig Tree	S 25° 54.572'	E 31° 1.597'	Lowe, 1999	SAF 115
SAF 36-57	Massive black cht.	Hooggenoeg	S 25° 56.633'	E 30° 53.117'	Lowe, 1999	SAF 36
SAF 483-1	Lam. black cht.	Mendon	S 25° 54.517'	E 31° 3.217'	This study	Barite W
MW-59-8	Lam. black cht.	Hooggenoeg	S 25° 57.767'	E 31° 1.300'	Walsh, 1989	MW-59
SAF 518-15	Lam. grey. sil. sed.	Mendon	S 25° 54.750'	E 31° 3.081'	This study	Barite W
SAF 518-30	Lam. grey. sil. sed.	Mendon	S 25° 54.750'	E 31° 3.081'	This study	Barite W
SAF 186-65	BFC	Mendon	S 25° 55.026'	E 30° 56.089'	This study	SAF 186
SAF 186-66	BFC	Mendon	S 25° 55.026'	E 30° 56.089'	This study	SAF 186
SAF 186-67	BFC	Mendon	S 25° 55.026'	E 30° 56.089'	This study	SAF 186
SAF 521-12	Lam. ferr. cht.	Fig Tree	S 25° 54.037'	E 31° 0.361'	This study	Umba Umba
SAF 186-62	Silicified ash	Fig Tree	S 25° 55.026'	E 30° 56.089'	This study	SAF 186
SAF 483-9	White sil. sed.	Mendon	S 25° 54.517'	E 31° 3.217'	This study	Barite W

Supplementary Table S4 – Matrix/cement composition and abundance from intraclast breccia point count analyses

Sample	Carb. Matrix (%)	Microqtz matrix + cement (%)	Total matrix + cement (%)	Ratio of carb. to microquartz matrix	Breccia type classification ^a
BH-03-2	18	13	31	1.5	S
BHR-01-07	8.8	24	32	0.4	L
BHR-01-08	5.8	34	40	0.2	S
BHR-01-09	4	31	35	0.1	S
BHR-02-17	5.3	26	32	0.2	S
BM-1-2	8.5	31	39	0.3	S
BM-1-3	3.3	34	37	0.1	S
BS-02-18	14	20	34	0.7	S
BS-02-19	13	24	37	0.5	B
BS-03-12	14	40	53	0.3	B
BS-03-14	44	19	64	2.3	B
BS-03-21	5.3	40	45	0.1	B
CQ-01-02	9.3	27	36	0.3	B
CQ-01-04	28	10	38	2.8	S
SAF 186-10	6	37	43	0.2	S
SAF 186-16	14	31	45	0.4	S
SAF 186-19	3.3	35	39	0.1	L
SAF 186-20	16	38	54	0.4	B
SAF 186-21	1.3	25	26	0.1	L
SAF 186-6-2	3	20	23	0.2	S
SAF 186-70-1	5.8	33	39	0.2	L
SAF 186-71	4.3	27	31	0.2	L
SAF 186-79	41	15	56	2.7	L
SAF 186-93-1	8.3	21	30	0.4	S
SAF 187-5	3.8	22	26	0.2	L
SAF 521-25	25	9.3	35	2.7	S
SAF 625-1	17	13	30	1.3	S
SAF 625-4	13	26	39	0.5	B
SAF 625-8	12	19	31	0.6	S
Mean (all)	12	26	38	0.7	
Mean (S)	11	23	35	0.8	
Mean (L)	9.7	26	35	0.5	
Mean (B)	16	30	47	0.7	

^aS – dominated by silica granules, granule aggregates, and chert bands (see Fig. 16a-b); L – dominated by laminated carbonaceous intraclasts (see Fig. 16d); B – dominated by black chert intraclasts (see Fig. 16d).

Supplementary Table S5 – Intraclast breccia point count data

Sample	Strat position (m)	Meas. top/bottom	Simple grains	Composite grains	Laminated intraclasts	Accretionary lapilli	Volcanic grains	Aggregates of accretionary lapilli	Silica granules	Aggregates of silica granules	Carb. matrix	Microquartz matrix/cement	Monocrystalline quartz	Impact spherule	White chert band intraclast	Opaque mineral	Black chert intraclast	Breccia type classification ^a
BH-03-2	11.3	top	43	8	0	0	1	0	13	202	73	50	0	0	3	0	7	S
BHR-01-07	1	bottom	23	54	48	0	5	0	7	16	35	94	0	0	118	0	0	L
BHR-01-08	1	bottom	21	68	0	0	5	0	7	39	23	137	0	0	96	4	0	S
BHR-01-09	1.5	bottom	12	43	77	1	51	1	12	19	16	125	0	0	42	1	0	S
BHR-02-17	1.75	top	23	21	14	0	21	0	31	66	21	105	0	0	81	1	16	S
BM-1-2	2.2	top	1	1	5	0	73	0	41	91	34	122	0	0	24	0	8	S
BM-1-3	2.2	top	7	3	3	0	98	0	9	24	13	136	1	0	102	0	4	S
BS-02-18	0.46	bottom	39	23	0	0	6	0	26	41	55	80	0	0	72	2	56	S
BS-02-19	0.24	bottom	17	7	0	0	58	0	4	3	52	96	0	0	18	0	145	B
BS-03-12	0.45	bottom	50	12	2	0	25	0	9	13	54	158	0	0	23	0	54	B
BS-03-14	1	bottom	46	7	1	0	17	0	27	0	177	77	0	0	7	0	41	B
BS-03-21	0.45	bottom	8	4	0	0	8	0	11	25	21	159	0	0	29	0	135	B
CQ-01-02	7.8	bottom	38	21	35	0	12	0	8	19	37	108	0	0	34	2	86	B
CQ-01-04	15	bottom	64	6	0	0	14	0	46	77	110	40	0	0	35	1	7	S
SAF 186-10	23.13	bottom	10	7	1	0	5	0	8	15	24	149	0	0	177	0	4	S
SAF 186-16	7.15	bottom	41	6	5	0	6	0	4	13	55	125	0	0	112	1	32	S
SAF 186-19	0.54	bottom	12	7	82	0	81	1	3	5	13	141	0	0	11	0	44	L
SAF 186-20	0.62	bottom	39	25	8	0	52	0	9	8	64	150	0	0	13	0	32	B

SAF 186-21	0.82	bottom	7	6	155	0	98	0	15	0	5	99	1	0	9	0	5	L
SAF 186-6-2	27.75	bottom	20	11	3	0	15	0	1	1	12	78	0	0	251	0	8	S
SAF 186-70-1	1.13	bottom	30	10	34	0	121	1	8	19	23	132	0	0	16	0	6	L
SAF 186-71	1.44	bottom	65	18	55	0	38	0	6	12	17	106	0	0	62	2	19	L
SAF 186-79	6.2	bottom	44	33	61	0	13	0	9	12	163	60	0	0	4	1	0	L
SAF 186-93-1	1.5	bottom	19	14	11	0	34	2	5	20	33	85	0	0	167	0	10	S
SAF 187-5	0.85	bottom	47	2	99	0	102	0	4	0	15	89	0	1	10	1	30	L
SAF 521-25	1	top	41	22	0	0	2	0	13	56	101	37	0	0	125	2	1	S
SAF 625-1	2.8	bottom	32	13	26	0	48	0	2	2	67	53	0	0	120	2	35	S
SAF 625-4	2.4	bottom	36	7	7	0	39	0	4	0	50	104	0	0	3	47	103	B
SAF 625-8	5.65	bottom	24	32	13	0	13	0	19	16	49	76	0	0	152	0	6	S

^aS – dominated by silica granules, granule aggregates, and chert bands (see Fig. 16a-b); L – dominated by laminated carbonaceous intraclasts (see Fig. 16d); B – dominated by black chert intraclasts (see Fig. 16d).

Supplementary Table S6 – Rare earth element concentrations (ppm)

Sample	SAF-521-3	SAF-521-10	SAF-199-10	SAF 518-15	SAF 518-30	SAF-521-12	SAF 186-65	SAF-186-67	SAF-186-62
Lithology	BBWC	BBWC	BBWC	Lam. grey	Lam. grey	Lam. ferr.	BFC	BFC	Silicified ash
La	0.38	1.11	1.37	11.21	6.47	1.17	4.12	2.15	202.93
Ce	0.67	1.81	2.17	8.33	11.23	2.02	7.80	3.74	201.40
Pr	0.07	0.19	0.25	1.91	1.16	0.21	0.90	0.42	38.94
Nd	0.26	0.70	0.96	5.68	3.74	0.85	3.41	1.67	144.37
Sm	0.06	0.16	0.17	1.03	0.55	0.21	0.78	0.39	28.01
Eu	0.02	0.05	0.05	0.25	0.17	0.07	0.27	0.20	6.30
Gd	0.06	0.16	0.12	0.83	0.66	0.23	0.93	0.51	21.54
Tb	0.01	0.03	0.02	0.14	0.14	0.04	0.17	0.10	3.09
Dy	0.07	0.17	0.13	0.86	1.07	0.25	1.18	0.75	17.21
Y	0.53	1.18	0.91	4.60	7.26	1.89	7.49	5.53	92.86
Ho	0.02	0.03	0.03	0.18	0.25	0.05	0.27	0.18	3.22
Er	0.04	0.10	0.09	0.51	0.74	0.16	0.78	0.53	8.03
Tm	0.01	0.02	0.01	0.08	0.11	0.02	0.12	0.08	1.08
Yb	0.05	0.10	0.10	0.50	0.69	0.16	0.79	0.54	6.63
Lu	0.01	0.02	0.02	0.08	0.11	0.02	0.12	0.09	0.98